PHYSICAL REVIEW A **67**, 010702(R) (2003)

Measurements of the ionization of atomic hydrogen by 17.6-eV electrons

Jochen Röder*
Infineon Technologies, Balanstrasse 73, 81541 Munich, Germany

Mark Baertschy†
Physics Department, University of Colorado at Denver, Denver, Colorado 80217-3364

Igor Bray‡
Centre for Atomic, Molecular, and Surface Physics, School of Mathematical and Physical Sciences, Murdoch University, Perth 6150, Australia

(Received 28 March 2002; revised manuscript received 25 July 2002; published 29 January 2003)

We report triply differential measurements of atomic hydrogen ionization by 17.6-eV electrons, with the outgoing electrons both having 2 eV energy. These measurements supersede some of the existing data. The complete set is critically analyzed and is found to be much more internally consistent than before, thereby providing one of the most stringent tests for theory to date. Comparison with the calculations from the exterior complex scaling and convergent close-coupling theories shows excellent overall agreement in both shapes and magnitude.

DOI: 10.1103/PhysRevA.67.010702 PACS number(s): 34.50.Fa

Triply (fully) differential cross sections (TDCS) for near threshold electron-impact ionization of atomic hydrogen were first measured by Schlemmer *et al.* [1]. Particular emphasis was put on the qualitative difference between $(e,2e)$ for He and H targets at 4 eV excess energy. That analysis was restricted to coplanar geometries with two 2-eV outgoing electrons, and a constant angular separation of $\theta_{AB}=180°$ between the two detectors. A more comprehensive set of measurements of the coplanar, equal-energy-sharing TDCS for 17.6-eV e-H ionization was presented by Brauner *et al.* [2]. This included data for geometries where the position of one detector was fixed at $\theta_A=60°$ and 140°, as well as data for $\theta_{AB}=150°$. The so-called coplanar (doubly) symmetric geometry, where $\theta_A=-\theta_B$ denotes that the detectors are always positioned symmetrically (one on either side) about the incident electron beam, was presented by Whelan *et al.* [3]. Additional data for $\theta_{AB}=90°$, 100°, and 120° were presented by Röder *et al.* [4].

These measurements were all relative, so the data were reported in arbitrary units. However, the experiments were designed such that the data for all geometries should be internormalized, i.e., the data describe a single surface as a function of θ_A and θ_B, whose overall, absolute value can then be determined by knowing the absolute value of a single point. In other words, one should be able to use a single scaling factor to convert all of the surface from the original arbitrary units to some set of known units.

The difficult task of putting the e-H TD cross-section measurements on the absolute scale was reported by Röder *et al.* [5], who put the $\theta_{AB}=180°$ slice on an absolute scale for the 15.6- and 17.6-eV incident electron energies, and thereby allowing all of the measured 15.6- and 17.6-eV relative TDCS to be put on an absolute scale.

However, for some geometries, the original 17.6-eV data [2] were found not to be sufficiently accurate and were subsequently remeasured and reanalyzed, but not published [6]. Independently, the problems with the data were highlighted by Bray [7]. Since data for all geometries were intended to be internormalized, the intersection of two different geometries should provide a common point that serves as a check of internal consistency. In the previously published data, the intersections between different geometries exhibit significant inconsistencies in the data. This indicates that there were problems with the internormalization procedure and/or stability in the experiment.

Here we present the previously unpublished most reliable data currently available for the coplanar TDCS (with each outgoing electron having 2 eV energy) for the electron-impact ionization of atomic hydrogen by 17.6-eV electrons. This includes improved measurements for the $\theta_A=-20°$, 60°, 140°, and $\theta_{AB}=150°$ geometries. We also present previously published data for $\theta_A=-\theta_B$ and $\theta_{AB}=90°$, 100°, 120°, 180° and check the internal consistency of the complete set of measurements. The old less accurate data are also presented to make it visually clear as to which of the original data require replacing and which are unaltered. The experimental data are compared with the most recent results of the exterior complex scaling (ECS) theory [8] and the convergent close-coupling (CCC) theory [9]. We shall begin with the discussion of the experiment and subsequently consider comparison with theory.

We present the revised data for the symmetric geometry (open squares) in Fig. 1, the fixed θ_A geometries (open circles) in Fig. 2, and the fixed θ_{AB} geometries (open triangles) in Fig. 3. We use light solid symbols for the data that have been previously used, but have now been superseded.

Points of intersection between two different geometries provide a means of checking the internal consistency of the

*Electronic address: jochen.roeder@infineon.com
†Electronic address: mbaertsc@carbon.cudenver.edu
‡Electronic address: I.Bray@murdoch.edu.au

 ©2003 The American Physical Society

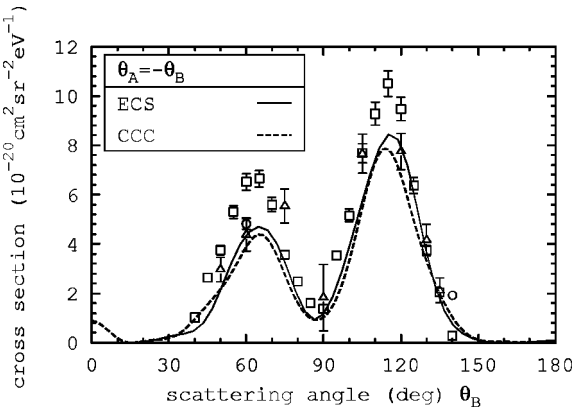

FIG. 1. Triply differential cross section for 17.6-eV electron impact ionization of atomic hydrogen with 2-eV outgoing electrons. The geometry considered is the (doubly) symmetric coplanar, where the two detectors are on opposite sides of the incident beam. Data obtained specifically for this geometry (squares) are plotted together with intersecting points of other geometries, see text. The ECS and CCC theories are given by Baertschy *et al.* [8] and Bray [9], respectively.

data. Since the data for each geometry were measured independently, the agreement between data points taken from different geometries at a point of intersection serves as a measure of how internally consistent the complete data set is. In each figure we show, where available, data from other geometries at the points of intersection. Throughout the figures we maintain consistency in the symbols used to denote data taken for the specific geometries. For instance, in Fig. 1 the primary data are for the symmetric geometry denoted by open squares, the open circles are data for intersecting points with the fixed θ_A geometries shown in Fig. 2, and the open triangles are data for intersecting points with the fixed θ_{AB} geometries shown in Fig. 3.

As can be seen from Fig. 1 there are data available for eight different points of intersection between the symmetric geometry and the various fixed θ_{AB} geometries. The largest discrepancy between the symmetric geometry data and the fixed θ_{AB} data is at $\theta_B=75°$, where the data point from $\theta_{AB}=150°$ is around two standard deviations higher. On the other hand, the other intersecting point of the $\theta_{AB}=150°$ geometry, at $\theta_B=\pm 105°$ ($+$ in Fig. 1 and $-$ in Fig. 3), agrees perfectly with the point from the symmetric geometry. There is also a discrepancy at $\theta_B=60°$ between the symmetric geometry data point and the corresponding one from $\theta_{AB}=120°$, except in this case the fixed θ_{AB} point is lower. The other intersecting point from $\theta_{AB}=120°$ (at $\theta_B=120°$) is also a little lower. We can compare the $\theta_B=60°$ point from the symmetric geometry with the $\theta_B=-60°$ point from the $\theta_A=60°$ geometry shown in Fig. 2. Here, the fixed θ_A point compares well with the corresponding point from the $\theta_{AB}=120°$ geometry, but less so with the symmetric geometry. Comparison between the symmetric geometry and a fixed θ_A geometry is possible at another point. This point of intersection is $\theta_B=140°$ in Fig. 1 and $\theta_B=-140°$ for $\theta_A=140°$ in Fig. 2. Here the discrepancy is quite large, but it should be pointed out that at this point the cross section is very small

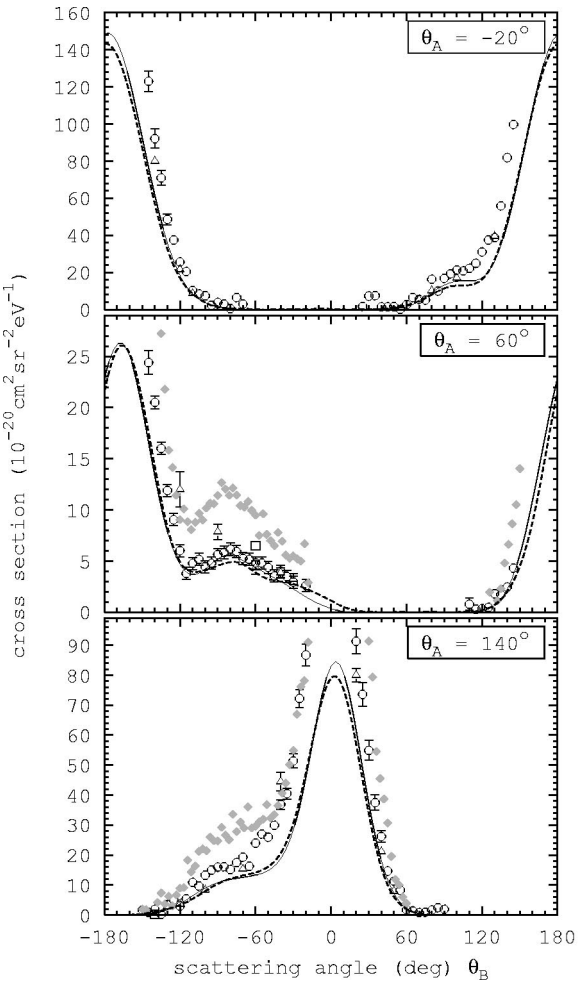

FIG. 2. Same as for Fig. 1, except showing all data obtained specifically for various fixed θ_A geometries (open circles). The old (see text) superseded data are shown as light solid symbols.

compared to the other values measured for the $\theta_A=140°$ geometry.

The entire set of new and old data for the fixed θ_A geometries along with a large number of intersecting points from the fixed θ_{AB} and symmetric geometries is presented in Fig. 2. The fixed $\theta_A=60°$ and $\theta_A=140°$ geometries were remeasured, while the $\theta_A=-20°$ geometry was also measured as a check of consistency and to provide extra data in the region where the TDCS are particularly large. Overall, we see good consistency between the fixed θ_A data (circles) and the fixed θ_{AB} data (triangles) shown in Fig. 3. The minor exceptions to this occur for the $\theta_A=60°$ geometry at $\theta_B=-120°$ and $-90°$. The intersecting points come from the $\theta_{AB}=180°$ and $\theta_{AB}=150°$ geometries, respectively. The discrepancy with the point at $\theta_B=-60°$ from the symmetric geometry has already been noted above. In general, we see that the internal consistency of the new dataset is substantially superior than with the old dataset presented here.

The complete set of fixed θ_{AB} data is presented in Fig. 3. Only the data for fixed $\theta_{AB}=150°$ [2] were found to require modification. They were found not to be correctly internormalized with the fixed $\theta_{AB}=180°$ data. Correcting this error

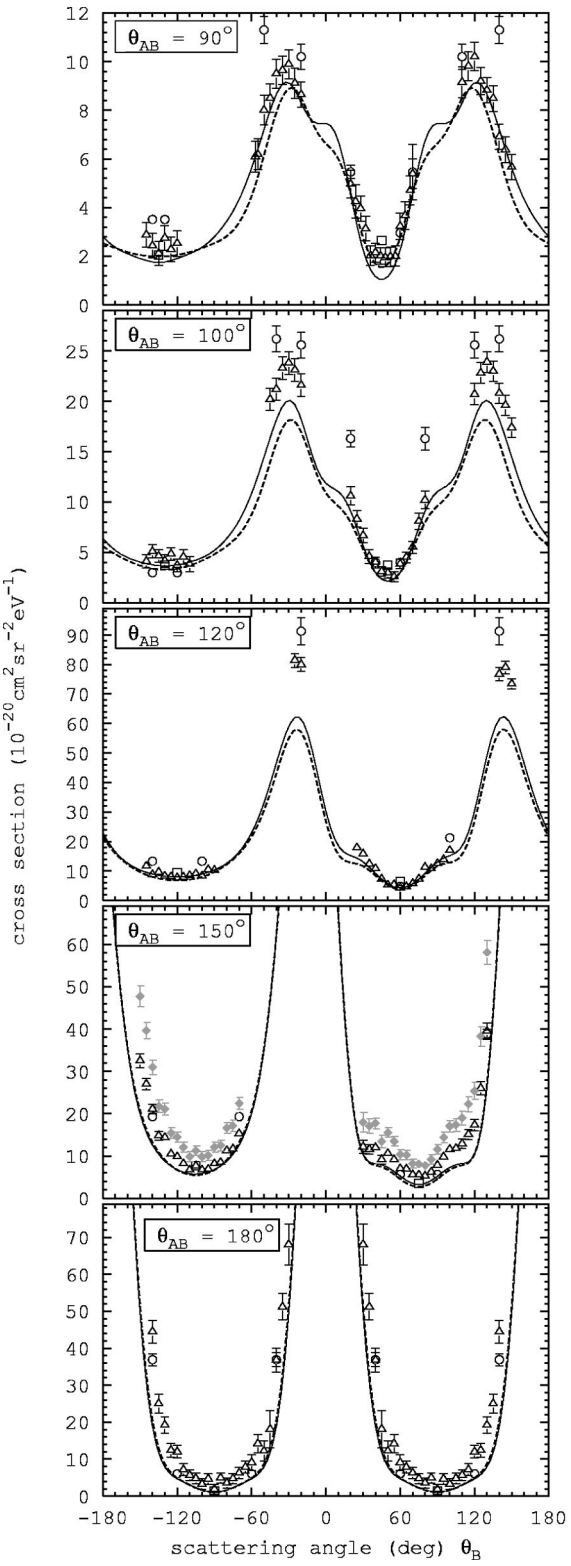

FIG. 3. Same as for Fig. 1, except showing all data obtained specifically for various fixed θ_{AB} geometries (open triangles). The superseded data (see text) are shown in light solid symbols.

has the effect of scaling the original $\theta_{AB}=150°$ data by 0.68 thereby making them more consistent with the data for other geometries. Starting with the $\theta_{AB}=90°$ data, for which the cross sections are the smallest, we see some discrepancy at the equivalent $\theta_B=-50°$ and $\theta_B=140°$ points. Here the intersecting point $\theta_B=50°$ from the $\theta_A=140°$ geometry (see Fig. 2) lies above the corresponding $\theta_{AB}=90°$ point. Even so, this is a substantially improved situation compared to that identified earlier, see Fig. 4 of Bray [7]. The equivalent points $\theta_B=20°$ and $\theta_B=80°$ of the $\theta_{AB}=100°$ geometry are noticeably different from the $\theta_B=80°$ point (circles) of the $\theta_A=-20°$ data. In the latter geometry the fluctuation in the data near $\theta_B=80°$, see Fig. 2, is comparable to these differences, suggesting this to be the source of the discrepancy. The new fixed $\theta_{AB}=150°$ data are strongly supported by the intersecting points at $\theta_B=-140°$ and at $\theta_B=130°$. The $\theta_{AB}=180°$ geometry is particularly interesting because these data should be symmetric about $\theta_B=0$ and $\theta_B=\pm 90°$. In the last panel of Fig. 3 the symmetry in the data about 0° (and $\pm 180°$), owing to the overall cylindrical symmetry of the system, was produced artificially by duplication. However, the symmetry about $\pm 90°$ does provide a means of checking the internal consistency of just the $\theta_{AB}=180°$ data, in that it corresponds to permuting the detectors. Comparing the $\theta_B=40°$ and 140° data is made simple by a common reference point (circles) from the $\theta_A=140°$ geometry. What we see is that at $\theta_B=40°$, the $\theta_{AB}=180°$ and $\theta_A=140°$ data are in excellent agreement, but at $\theta_B=140°$, the $\theta_{AB}=180°$ point is noticeably higher. This lack of symmetry in the $\theta_{AB}=180°$ data gives an indication of the amount of relative error in the measurements. Although this and other discrepancies indicate imperfections in the data, the overall internal consistency in the data is much improved over the situation that existed earlier [7].

We now turn to the comparison with theory. The latest results from the ECS and CCC theories are used for comparison with experiment. The ECS-calculated TDCS are based on the evaluation of the underlying amplitudes [8], and supersede those based on the flux method [10,11]. The presented CCC-calculated TDCS [9] also supersede the earlier calculations [7]. The latter used Laguerre basis sizes $N_l=20-l$ with the exponential falloffs $\lambda_l \approx 0.8$ varied to ensure that one pseudostate had exactly 2 eV energy for each l. These calculations were at the limit of the computational resources available to the CCC theorists at the time. The presented calculation has $N_l=50-l$ with $\lambda_l=2$. The larger bases allow for relatively accurate interpolations of the complex scattering amplitudes. It is the systematic variation of the λ_l, necessary in the much smaller calculations, that has led to the apparent convergence to the wrong result for equal-energy-sharing cases [7]. A case study for 27.2 eV incident electron energy discusses the convergence of the CCC-calculated TDCS for unequal- and equal-energy sharing [12]. In addition, 25-eV e-H ionization has been recently discussed in a review of the CCC theory applications [13].

The TDCS from the ECS theory were obtained from wave functions calculated out to distances of $130a_0$, which include components for total angular momentum up to $L=9$ [8]. The CCC calculations treat the two electrons on a different footing. The projectile space is treated using plane waves extending out to arbitrarily large distances, while the extent of the target-space electron is constrained by the number of oscil-

lations induced by the basis size N_l and the electron energy. Thus, low-energy electrons extend a good deal further in space than do the higher-energy ones. The usage of orbital angular momenta is also a little different in the CCC and ECS theories. In CCC we specify a target-space $l_{\max}$ ($=5$ presently) and the maximum partial wave $L_{\max}$ ($=10$ presently). In ECS we set $L_{\max}=9$ and used as many (l_1,l_2) pairs for each value of L as necessary to converge the coupled equations [11].

The two theories reproduce the shapes of the measured TDCS very well, but generally are about 30% lower than the experiment. Given the stated uncertainty of 40% in the absolute value determination [5], it is reasonable to argue that the theory yields quantitative agreement with the experiment. There is some evidence that the CCC theory is struggling to accurately calculate the TDCS for geometries where the cross section is particularly small. See, for example, the forward angles of Fig. 1. The TDCS arise from a coherent combination of the scattering amplitudes that must be particularly accurate if their coherent combination is to yield near zero. Reliance on interpolation of complex numbers across the secondary energy range makes this computationally particularly challenging.

There have been many other wide-varying theories applied to the problem, see Röder *et al.* [4], for example. One that, in our view, is particularly worth noting is the distorted partial wave (DPW) theory of Pan and Starace [14], which evaluates only the $\theta_{AB}=180°$ geometry. The 17.6-eV DPW-calculated TD cross section presented by Röder *et al.* [5] is indistinguishable from the ECS and CCC ones plotted in the bottom panel of Fig. 3, thereby lending further support to the accuracy of both theory and experiment at this energy. In addition, the 15.6-eV DPW-calculated $\theta_{AB}=180°$ TDCS [5] are consistent with the subsequent TDCS from the CCC [15] and ECS [8] theories, both of which are able to reproduce the full set of the measured geometries, but only after the experimental absolute values [5] are reduced by a factor of 2. Thus we have three independent theories suggesting that the measured 15.6-eV TD cross section has the mean estimate for the absolute value too high by a factor of 2.

In conclusion, the measurements reported here supersede some of the existing measurements for 17.6-eV e-H ionization, and the new complete set is now far more consistent, as a whole, than it was previously. Satisfactory absolute agreement with ECS, CCC, and DPW theory is found. However, we do note that a factor of 2 discrepancy in the absolute values at 15.6 eV remains, and a lack of availability of absolute e-H TDCS at other energies with equal-energy-sharing kinematics suggests that the experimental establishment of the absolute cross sections for low to intermediate energy e-H ionization is as important as ever.

The authors thank Bill McCurdy and Tom Rescigno. I.B. acknowledges the support of Murdoch University and the Australian Research Council. M.B. acknowledges support from the U.S. Department of Energy Office of Basic Energy Science, Division of Chemical Sciences.

[1] P. Schlemmer, T. Rösel, K. Jung, and H. Ehrhardt, Phys. Rev. Lett. **63**, 252 (1989).
[2] M. Brauner, J.S. Briggs, H. Klar, J.T. Broad, T. Rösel, K. Jung, and H. Ehrhardt, J. Phys. B **24**, 657 (1991).
[3] C.T. Whelan, R.J. Allan, J. Rasch, H.R.J. Walters, X. Zhang, J. Röder, K. Jung, and H. Ehrhardt, Phys. Rev. A **50**, 4394 (1994).
[4] J. Röder, J. Rasch, K. Jung, C.T. Whelan, H. Ehrhardt, R.J. Allan, and H.R.J. Walters, Phys. Rev. A **53**, 225 (1996).
[5] J. Röder, H. Ehrhardt, C. Pan, A.F. Starace, I. Bray, and D.V. Fursa, Phys. Rev. Lett. **79**, 1666 (1997).
[6] J. Röder, Ph. D. thesis, University of Kaiserslautern, Germany, 1996 (unpublished).
[7] I. Bray, J. Phys. B **33**, 581 (2000).
[8] M. Baertschy, T.N. Rescigno, and C.W. McCurdy, Phys. Rev. A **64**, 022709 (2001).
[9] I. Bray, Phys. Rev. Lett. **89**, 27320 (2002).
[10] T.N. Rescigno, M. Baertschy, W.A. Isaacs, and C.W. McCurdy, Science **286**, 2474 (1999).
[11] M. Baertschy, T.N. Rescigno, W.A. Isaacs, X. Li, and C.W. McCurdy, Phys. Rev. A **63**, 022712 (2001).
[12] I. Bray, J. Phys. B (unpublished).
[13] I. Bray, D.V. Fursa, A.S. Kheifets, and A.T. Stelbovics, J. Phys. B **35**, R117 (2002).
[14] C. Pan and A.F. Starace, Phys. Rev. A **45**, 4588 (1992).
[15] I. Bray, J. Phys. B **32**, L119 (1999).